Optically monitoring voltage in neurons by photo-induced electron transfer through molecular wires

Evan W. Miller[a], John Y. Lin[a], E. Paxon Frady[b], Paul A. Steinbach[a,c], William B. Kristan, Jr.[d], and Roger Y. Tsien[a,c,e,1]

[a]Department of Pharmacology, [b]Neurosciences Graduate Group, [d]Division of Biological Sciences, [e]Department of Chemistry and Biochemistry, and [c]Howard Hughes Medical Institute, University of California at San Diego, La Jolla, CA 92093

Contributed by Roger Y. Tsien, December 21, 2011 (sent for review November 26, 2011)

Fluorescence imaging is an attractive method for monitoring neuronal activity. A key challenge for optically monitoring voltage is development of sensors that can give large and fast responses to changes in transmembrane potential. We now present fluorescent sensors that detect voltage changes in neurons by modulation of photo-induced electron transfer (PeT) from an electron donor through a synthetic molecular wire to a fluorophore. These dyes give bigger responses to voltage than electrochromic dyes, yet have much faster kinetics and much less added capacitance than existing sensors based on hydrophobic anions or voltage-sensitive ion channels. These features enable single-trial detection of synaptic and action potentials in cultured hippocampal neurons and intact leech ganglia. Voltage-dependent PeT should be amenable to much further optimization, but the existing probes are already valuable indicators of neuronal activity.

Fluorescence imaging can map the electrical activity and communication of multiple spatially resolved neurons and thus complements traditional electrophysiological measurements (1, 2). Ca^{2+} imaging is the most popular of such techniques, because the indicators are well-developed (3–6), highly sensitive (5, 6), and genetically encodable (7–13), enabling investigation of the spatial distribution of Ca^{2+} dynamics in structures as small as dendritic spines and as large as functional circuits. However, because neurons translate depolarizations into Ca^{2+} signals via a complex series of pumps, channels, and buffers, fluorescence imaging of Ca^{2+} transients cannot provide a complete picture of electrical activity in neurons. Observed Ca^{2+} spikes are temporally low-pass filtered from the initial depolarization and provide limited information regarding hyperpolarizations and subthreshold events. Direct measurement of transmembrane potential with fluorescent indicators would provide a more accurate account of the timing and location of neuronal activity. Despite the promise of fluorescent voltage-sensitive dyes (VSDs), previous classes of VSDs have each been hampered by some combination of insensitivity, slow kinetics (14–16), heavy capacitative loading (17–21), lack of genetic targetability, or phototoxicity. Two of the more widely used classes of VSDs, electrochromic and FRET dyes, illustrate the problems associated with developing fast and sensitive fluorescent VSDs.

Electrochromic dyes respond to voltage through a direct interaction between the chromophore and the electric field (Scheme 1*A*). This Stark effect leads to small wavelength shifts in the absorption and emission spectrum. Because the electric field directly modulates the energy levels of the chromophore, the kinetics of voltage sensing occur on a timescale commensurate with absorption and emission, resulting in ultrafast (fs to ps) hypso- or bathochromic shifts many orders-of-magnitude faster than required to resolve fast spiking events and action potentials in neurons. This small wavelength shift dictates that the fluorescence signal can be best recorded at the edges of the spectrum, where intensity varies most steeply as a function of wavelength. The largest linear responses are −28% ΔF/F per 100 mV (22), although more typical values are ∼10% per 100 mV (23, 24). Photo-induced electron transfer (PeT)-based Ca^{2+} probes, such as fluo-3, give ΔF/F values of up to 150% for action potentials in cultured hippocampal neurons (25). Therefore, although electrochromic dyes can keep pace with fast voltage oscillations in neurons, their insensitivity limits the systems in which these dyes can successfully report on voltage changes.

FRET-based voltage sensors use lipophilic anions that intercalate into the cellular membrane and distribute between the inner and outer leaflets depending upon the transmembrane potential (Scheme 1*B*). The Nernstian distribution is monitored by a second fluorophore immobilized on one side of the membrane, which undergoes FRET preferentially with the mobile anions on the same side of the membrane. Translocation of the lipophilic anion through the lipid bilayer governs the kinetics of voltage sensing, which can be in the millisecond range. Although these two-component systems can give large changes in intensity (5–34%) (21) or ratio (80% per 100 mV) (15), the slow translocation of mobile charges in the plasma membrane introduces a capacitative load and hampers the ability of the reporter to monitor fast changes.

To combine the best features of electrochromic and FRET-based VSDs, we have now tested a unique mechanism for voltage sensing, PeT through molecular wires. In these PeT sensors, a fluorescent reporter connects to an electron-rich quencher via a molecular wire, which minimizes the exponential distance dependence of intramolecular electron transfer (26) and allows efficient electron transfer over a major fraction of the thickness of the plasma membrane. At resting or hyperpolarized potentials, the transmembrane electric field promotes electron transfer from the quencher to the excited-state fluorophore through the molecular wire, quenching fluorescence (Scheme 1*C*). Depolarization reverses the electric field, hinders electron transfer, and brightens fluorescence (27), just as Ca^{2+} binding dequenches indicators like fluo-3 (28). Electron transfer occurs within pico- to nanoseconds after photon absorption and returns to its initial state within a microsecond (26, 29), slower than the electrochromic mechanism but essentially instantaneous on a biological timescale. Because electron transfer reverses quickly and is driven by photon absorption rather than membrane potential changes, capacitative loading should be negligible, as calculated in the *SI Appendix*. A full electronic charge traverses a Marcus-type thermal activation barrier to sense a large fraction of the membrane voltage, making voltage sensitivity high (30). Quenching of the fluorescent reporter by the electron-rich donor modulates the fluorescence quantum yield independent of wavelength, permitting efficient use of photons for excitation and emission, allowing lower light levels or dye concentrations to be used. We report here the design, synthesis, and application of the VoltageFluor (VF) family of fluorescent sensors as molecular wire PeT-based probes for voltage imaging in neurons.

Author contributions: E.W.M., W.B.K., and R.Y.T. designed research; E.W.M., J.Y.L., E.P.F., and P.A.S. performed research; E.W.M., E.P.F., W.B.K., and R.Y.T. analyzed data; and E.W.M. and R.Y.T. wrote the paper.

The authors declare no conflict of interest.

Freely available online through the PNAS open access option.

[1]To whom correspondence should be addressed. E-mail: rtsien@ucsd.edu.

This article contains supporting information online at www.pnas.org/lookup/suppl/doi:10.1073/pnas.1120694109/-/DCSupplemental.

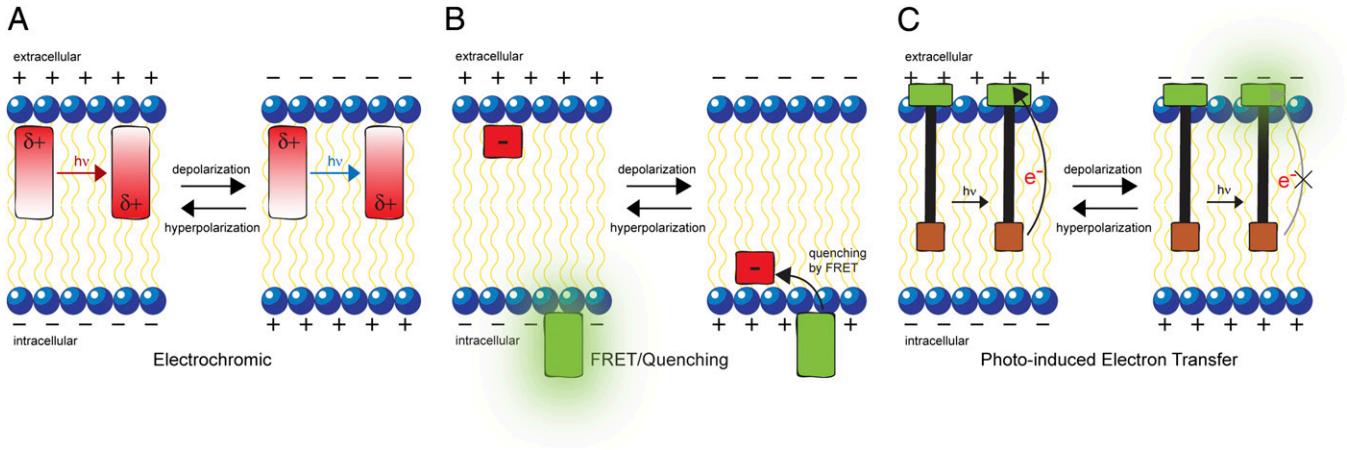

Scheme 1. Mechanisms of fluorescent voltage sensing. (*A*) Electrochromic VSDs sense voltage through the Stark effect, whereby the chromophore interacts directly with the electric field. Absorption of a photon significantly alters the excited state molecular dipole, which at hyperpolarizing potentials is stabilized (*Left*). At depolarizing potentials the charge shift inverted state is destabilized (*Right*). Changes in the energy levels of the chromophore result in small spectral shifts in the emission of the dye. (*B*) FRET-pair voltage sensors use lipophilic anions (red), which partition in a voltage-dependent fashion on the inner or outer leaflet of the membrane. Depolarization causes translocation of the anion, which can now quench the fluorescence of an immobilized fluorophore (green). (*C*) Molecular wire PeT VSDs depend upon the voltage-sensitive electron transfer from an electron-rich donor (orange) through a membrane-spanning molecular wire (black) to a fluorescent reporter (green). At hyperpolarizing potentials, the electric field is aligned antiparallel to the direction of electron transfer, resulting in efficient PeT and quenched fluorescence (*Left*). Depolarization aligns the electric field in the direction of PeT, decreasing the rate of electron transfer and increasing fluorescence (*Right*).

Results

Design and Synthesis of VF Sensors. Our initial voltage sensors incorporate dichlorosulfofluorescein as a membrane-impermeant fluorophore, a *p*-phenylenevinylene (PPV) molecular wire, and *N*, *N*-dimethyl- or dibutylaniline as an electron-rich quencher (Scheme 2). VF1.4.Cl comprises 2,7-dichlorosulfofluorescein connected via one vinylene unit to dibutylaniline (hence VF1.4.Cl). VF2.4.Cl adds a second PPV unit, and VF2.1.Cl features the same configuration, with methyl substituted in place of butyl groups.

Correct positioning of the fluorophore-wire donor within the membrane is vital to take advantage of the vectoral nature of the transmembrane electric field and electron transfer. First, the longitudinal axis of the molecular wire must be normal to the plane of the plasma membrane, to sample the full electric field. Second, dye molecules must all align in the same direction to avoid canceling out the electron transfer effect. Positioning the fluorophore at the extracellular leaflet of the membrane ensures fluorescence brightening upon depolarization; the opposite orientation of PeT would give fluorescence quenching upon depolarization.

The negatively charged sulfofluorescein will preclude dye internalization and force an orientation in which the fluorophore adsorbs to the outer leaflet of the plasma membrane, with the lipophilic molecular wire and alkyl aniline dangling into the lipid bilayer. As an intervening spacer, PPV molecular wires are an ideal choice because of their low attenuation values (26), synthetic tractability, and demonstrated ability to conduct current through lipid bilayers (31). Anilines are common PeT donors and the dialkyl groups should enhance uptake into the plasma membrane.

A modular synthetic design both allows for rapid generation of the voltage sensors and enables future derivatization (Scheme 2 and *SI Appendix*). Coupling of the molecular wire styrene unit **1**, available in one step from 4-di-butylaminobenzaldehyde, with iodo-functionalized dichlorosulfofluorescein **2** via a Pd-catalyzed Heck reaction gives VF1.4.Cl in good yield. An analogous reaction with molecular wire **3**, available in two steps from **1**, gives VF2.4.Cl in 70% yield. A parallel reaction beginning from styrene **4** furnishes VF2.1.Cl in good yield. All dyes feature emission and excitation profiles typical of dichlorofluoresceins (VF1.4.Cl: λ_{max} = 521 nm, ε = 93,000 $M^{-1}\cdot cm^{-1}$, λ_{em} = 534 nm, Φ = 0.24; VF2.4.Cl:

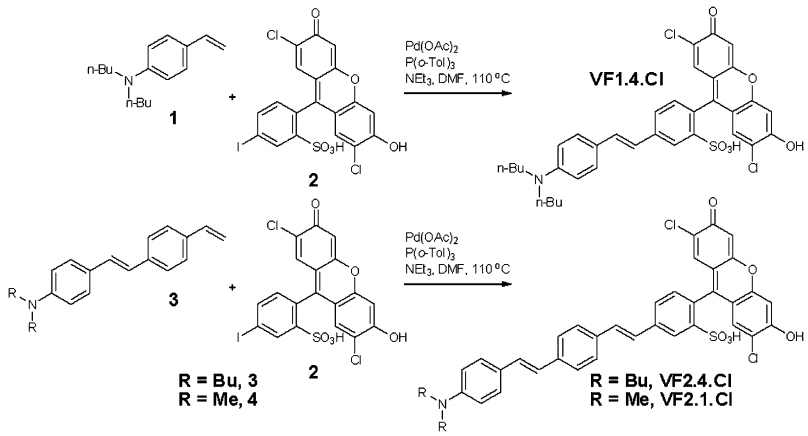

Scheme 2. Synthesis of VF probes.

λ_{max} = 522 nm, ε = 97,000 $M^{-1}{\cdot}cm^{-1}$, λ_{em} = 536 nm, Φ = 0.054; VF2.1.Cl: λ_{max} = 522 nm, ε = 98 000 $M^{-1}{\cdot}cm^{-1}$, λ_{em} = 535 nm, Φ = 0.057, 5 mM sodium phosphate, pH 9, 0.1% Triton X-100) (*SI Appendix*, Fig. S1). The dibutyl (VFx.4.Cl) dyes stain the cell membranes of HEK293 cells when loaded at a concentration of 2 μM for 15 min at 37 °C in buffer with 0.1% DMSO as cosolvent (Fig. 1*A*, and *SI Appendix*, Fig. S2). VF2.1.Cl requires even lower dye concentrations (100 nM) and gives bright staining of HEK cell membranes, which is likely to be because of the greater aqueous solubility of VF2.1.Cl compared with VF2.4.Cl in aqueous solution (*SI Appendix*, Fig. S2). The membrane retention of the second generation dyes (VF2.x.Cl) is in contrast to di-4-ANEPPS, which at the same loading conditions, shows significant uptake into internal membranes. The bleach rates of the probes were tested in HEK cells and compared with di-4-ANEPPS. The bleach rates for VF1.4.Cl, VF2.4.Cl, and VF2.1.Cl at 7 W/cm^2 were measured to be 3.9 ± 0.1 × 10^{-2} s^{-1}, 1.8 ± 0.1 × 10^{-2} s^{-1}, and 8.0 ± 0.1 × 10^{-3} s^{-1}, respectively. These results are two-, four-, and ninefold smaller than di-4-ANEPPS, which has a bleach rate, under identical illumination conditions, of 6.9 ± 0.1 × 10^{-2} s^{-1}.

Characterization of the Voltage Response of VF Sensors. We characterized the voltage sensitivity of all three indicators by making tight-seal whole-cell recordings of HEK293 cells stained with the VF sensors. Cells were voltage-clamped at −60 mV holding potential and sequentially stepped to depolarizing and hyperpolarizing potentials at 20-mV increments (Fig. 1*B*). For all three dyes, depolarizing steps produced fluorescence increases, whereas hyperpolarizing steps produced fluorescence decreases, in keeping with the proposed PeT mechanism. The fluorescence response is linear over the range of −100 mV to +100 mV (Fig. 1*C*), with voltage sensitivities ΔF/F per 100 mV of 20 ± 1% for VF1.4.Cl and 25 ± 1% for VF2.4.Cl. This statistically significant increase in voltage sensitivity ($P < 0.05$, two-tailed Student *t* test) is expected upon increasing the length of the molecular wire, and is 2.5- to 4-times more sensitive than di-4-ANEPPS, which, in our hands, gives sensitivities of between 6% and 10% ΔF/F per 100 mV. VF2.1.Cl shows fluorescence increases upon depolarization similar to VF2.4.Cl, with a voltage sensitivity of 27 ± 1% per 100 mV. This value is not significantly different from the sensitivity of VF2.4.Cl, suggesting that voltage sensitivity is largely determined by the length of the molecular wire and that the small increase in electron donating ability of the butyl relative to the methyl groups makes only a relatively small contribution to the increased voltage sensitivity of VF2.1.Cl. To investigate the speed of response of VF probes, we again made whole-cell recordings of cells stained with VF2.4.Cl, applied 100-mV depolarizing steps from a holding potential of −60 mV, and recorded both the electrophysiological signals and the optical signals. Fitting the electrophysiological and optical recordings gave identical time constants for both beginning and end of the pulse ($\tau_{ON,\ phys}$ = 139 ± 0.2 μs, $\tau_{ON,\ optical}$ = 138 ± 14 μs, $\tau_{OFF,\ phys}$ = 142 ± 0.4 μs, $\tau_{OFF,\ optical}$ = 147 ± 19 μs), showing that VF2.4.Cl and related sensors do not introduce any detectable lag in their fluorescence response to voltage, consistent with a PeT-based mechanism for voltage sensing (Fig. 2 *A* and *B*).

The fluorescence response of VF2.4.Cl to voltage changes is insensitive to the excitation wavelength, as is true for PeT-based probes, such as fluo-3 and Calcium Green-1. We assayed the wavelength dependence of VF2.4.Cl by changing the excitation wavelength in 5-nm steps and determined that the fluorescence response of VF2.4.Cl to a 100-mV depolarization from a holding potential of −60 mV varied only about 15% when testing wavelengths from 445 to 500 nm (Fig. 2*C*). In comparison, di-4-ANEPPS varies by nearly 100% over its excitation spectrum (32), and the PeT-based Ca^{2+} sensor, Calcium Green-1, varies by ~20% (*SI Appendix*, Fig. S3). These comparisons show that the wavelength independence of the voltage sensitivity is more consistent with PeT than a wavelength-shifting mechanism, such as electrochromism or solvatochromism (a wavelength shift because of alteration in local solvation).

PeT-based molecular wire sensors do not affect neuronal excitability by capacitative loading. We injected hyperpolarizing current into the Retzius cells of leech ganglia preparations and compared the time constants for these voltage steps in ganglia under different dye loading conditions. The ganglia were stained with dye at three times the working concentration [either VF2.1.Cl or diSBA-C_4-(3) (14)] and compared with unloaded cells. The presence of the translocating dye oxonol 413 substantially increases the capacitative load on the membrane, as measured by the increase in the RC time constant for the hyperpolarizing injection (Fig. 2*D*). On the other hand, ganglia loaded with VF2.1.Cl show no difference from control cells, demonstrating that molecular wire sensors place negligible capacitative load on the cell (Fig. 2*D*), confirming the predictions of the *SI Appendix*.

Detection of Action Potentials by VF2.4.Cl in Mammalian Neurons. To assess whether VF probes can detect action potentials in single trials, we used cultured rat hippocampal neurons. Bath application of 2 μM VF2.4.Cl showed bright cell staining limited to the cell membranes of neurons and their support cells (Fig. 3*A*). We then injected current into a neuron under whole-cell patch-clamp mode to trigger single action potentials and used a high-speed, back-illuminated EMCCD camera to track fast optical signals from VF2.4.Cl, enabling us to resolve action potentials in neurons in single sweeps (Fig. 3*B*). The optical trace matched the physiology trace and gave about a 20% ΔF/F increase in fluorescence and a 16:1 signal-to-noise ratio (SNR) in a single trial. The fact that VF2.4.Cl detected action potentials without spike-timed averaging suggests the possibility of measuring spontaneous action potentials in neurons at sites away from the recording pipette.

Monitoring Spontaneous Activity in Leech Ganglia with VF2.1.Cl. A more stringent test of the usefulness of the PeT-based VSD is to determine whether it can accurately measure subthreshold activity in heterogeneous preparations. For this test we used leech ganglia, because their neurons have been well studied using both

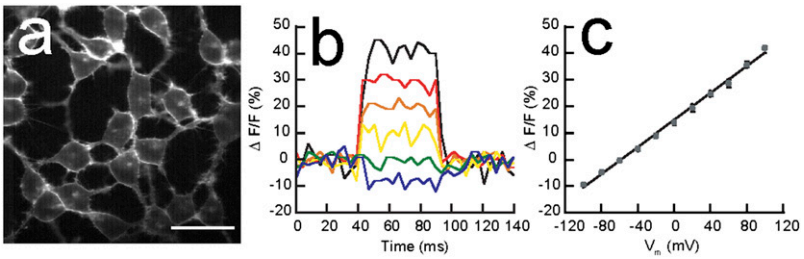

Fig. 1. Characterization of VF sensors in HEK cells. (*A*) Confocal image of HEK 293 cells stained with 2 μM VF2.4.Cl. (Scale bar, 20 μm.) (*B*) Fractional changes in VF2.4.Cl fluorescence during a series of voltage steps to +100 or −100 from a holding potential of −60 mV (40-mV increments). (*C*) Fractional changes in VF2.4.Cl fluorescence from *B* plotted against membrane potential for voltage changes from a holding potential of −60 mV. Each datapoint represents three to four separate measurements. Error bars are SEM.

electrophysiological and other VSD recordings (14, 33–35). We isolated a midbody ganglion and stained it with VF2.1.Cl for 15 min at 22 °C (Fig. 3*C*). Insertion of a sharp electrode (25 MΩ) into a Retzius cell to enabled recording of its spontaneous activity while simultaneously recording the fluorescence signals from the same cell. When sampling at a rate of 50 Hz, the optical recording (Fig. 3*D*, red trace) faithfully followed the subthreshold fluctuations in the electrical recording (black trace). The optically recorded spikes are truncated as a result of undersampling the optical signal; sampling at a higher rate (722 Hz) fully resolved the action potentials, but introduced a significant amount of sampling noise (*SI Appendix*, Fig. S4). Although the action potential was subsampled at just 50 Hz, there is still a reliable transient in the optical trace that indicates the time when an action potential occurs, which is often what is needed.

The PeT-based VSDs show significant improvement in speed and accuracy compared with FRET-based VSDs previously used for leech recordings (33, 36–38), which in turn had superseded electrochromic dyes (14). The improvement in the recording of membrane potential fluctuations is not the result of a greater sensitivity (the ΔF/F for both the FRET and PeT dyes is about 10% per 100 mV in leech recordings), but to a greater SNR. The PeT-based VSD produces a much brighter signal, one that is well above the photon noise levels of the dye and the dark noise level of the camera. Increasing the concentration of the FRET-based dye does increase its SNR, but the consequent increase in the cell's capacitance (Fig. 2*D*) makes the dye useless for recording either action potentials or synaptic potentials. Tests of the toxicity and bleaching of the PeT-based VSD similar to those performed on the FRET-based dyes (14) show that the PeT-based VSD has a slower rate of bleaching and is less toxic than the FRET-based dyes. Hence, considering all measures, the PeT-based VSD performs better than the FRET-based dyes (39).

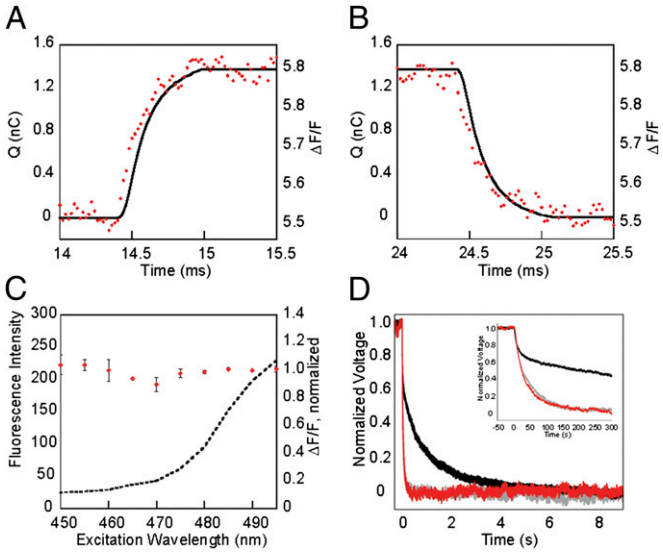

Fig. 2. Characterization of the speed, wavelength sensitivity, and capacitance of the VF2 fluorescence response. (*A*) Rising edge of a 100-mV depolarizing step from −60 mV in HEK cells stained with VF2.4.Cl. (*B*) Falling edge of the same step. Black, solid trace is the integrated current measured electrophysiologically; red points are the optical recording. Time constants are calculated by fitting a monoexponential equation to each side of the step. Traces are the average of 100 sequential trials. (*C*) Voltage sensitivity vs. excitation wavelength. The normalized response of VF2.4.Cl to a 100 mV depolarization from −60 mV in HEK cells is plotted in red, and the excitation spectrum in HEK cells is the dotted black line. Error bars are SEM for $n = 3$ experiments. (*D*) Measurement of capacitative loading in leech Retzius cells. Traces show the normalized voltage decay following hyperpolarizing current injection into Retzius cell stained with 3× VF2.1.Cl (red trace), 3× oxonol 413 (black trace), or nothing (gray trace). (*Inset*) An expanded time scale revealing no difference between cells stained with VF2.1.Cl and control cells.

Discussion

Optimal VSDs would have large, fast responses to changes in voltage, place little or no capacitative load on the membrane, photobleach slowly with minimal photodynamic damage, and would be synthetically tractable for rational chemical modification and genetic targetability. We believe that the VF family of PeT-based probes surpass previous VSD classes by these criteria. The three PPV molecular wire, PeT-based molecules we tested (VF1.4.Cl, VF2.4.Cl, and VF2.1.Cl) exhibit good membrane staining and 20–27% ΔF/F per 100-mV increases in fluorescence upon depolarization in HEK cells. These molecules possess the fast kinetics ($\tau_{ON/OFF}$ <<140 μs) and wavelength-independent voltage sensitivity consistent with a PeT mechanism for sensing voltage. Measurements of capacitance in leech neurons show that an insignificant amount of capacitative load is placed on the membrane. The advantages of PeT-based dyes over both electrochromic and FRET-based methods for optical voltage sensing are described below and summarized in Table 1. A fourth technique, making use of genetically encoded voltage sensors, offers a promising method for optically monitoring voltage changes because the fluorescent proteins can be targeted to cells of interest, thereby increasing the SNR of the fluorescence response. In practice, however, fluorescent protein voltage sensors suffer from low sensitivity [0.5% (40) to 10% Δ F/F per 100 mV (41)], nonlinear responses (42) and slow kinetics (tens to hundreds of milliseconds). Newer efforts have made use of proton translocation within bacterial rhodopsins (43), but although these show large voltage sensitivities, the response time is still in the millisecond range, quantum efficiencies are very low, and their expression limited to prokaryotic systems. Voltage-driven translocation of ions through the membrane will generally add much more capacitative load than electron translocation during transient excited states (44).

VSDs using a PeT-based molecular wire approach should be highly sensitive. Because a full electronic charge travels through a substantial fraction of the transmembrane voltage (11 Å for VF1.4.Cl, 17 Å for VF2.4.Cl and VF2.1.Cl, or 37% and 57% of the 30 Å low-dielectric constant core of the plasma membrane) the change in driving force for PeT is large. For example, a 100-mV depolarization changes the PeT driving force by 0.05 eV (one electron × half of 100-mV potential, or 0.05 V). Because PeT is a thermally controlled process, the value of 0.05 eV is large relative to the value of kT at 300 K (0.026 eV), yielding a large dynamic range between the rates of PeT at resting and depolarized potentials. FRET-based VSDs will have similar sensitivities; lipid-soluble mobile anions transverse distances calculated to be between 0.4 (16) and 0.6 (45) of the total membrane width, resulting in ΔG of ~0.05 eV for 100-mV depolarization, compared with a kT of 0.026 eV for the thermally activated process.

In contrast, electrochromic dyes have smaller ΔG values, 0.003 (46) to 0.02 (47) eV, and larger comparison energies. Because the interaction is a photochemically controlled process, the energy of the exciting photon is the comparison energy, which is 1.5–2 eV for dyes in the blue-to-green region of the spectrum. Therefore, PeT and FRET dyes have large changes in energy versus their comparison energy (0.05 eV vs. 0.026 eV), giving high sensitivities; electrochromic dyes have small changes compared with the excitation photon (0.003–0.02 eV vs. 2 eV), producing low voltage sensitivity.

The nature of the PeT mechanism also predicts that the kinetics of voltage sensing will be fast; forward electron transfer occurs on the nanosecond timescale as fluorescence is quenched, and back-electron transfer completes the cycle and occurs on a microsecond timescale or faster, meaning that the slow step, electron-hole recombination, finishes a full three orders-of-magnitude faster than an action potential. Electrochromic dyes

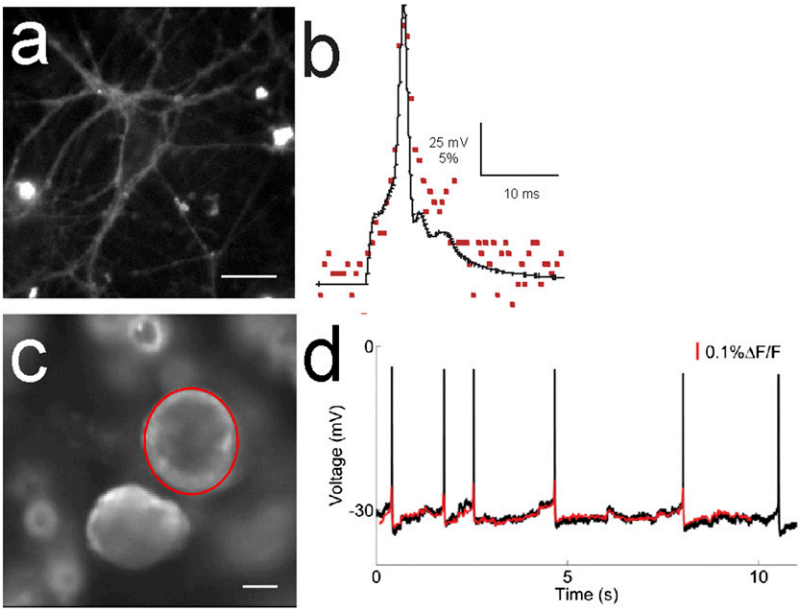

Fig. 3. VF2 dyes resolve action potentials in neurons. (*A*) Rat hippocampal neurons stained with 2 μM VF2.4.Cl for 15 min show strong membrane staining. (Scale bar, 20 μm.) (*B*) VF2.4.Cl can detected evoked action potentials in rat hippocampal neurons in single trials. The black trace is the recorded electrophysiology signal. Individual points represent the optical signal from VF2.4.Cl captured with a high speed EMCCD camera at a rate of 2 kHz. (*C*) Optical imaging of spontaneous activity in leech Retzius cells using the dye VF2.1.Cl. Desheathed midbody leech ganglion stained with 200 nM VF2.1.Cl for 15 min. Pixels within the region of interest (red circle around a single Retzius cell body) were averaged in each frame to produce the optical trace. (Scale bar, 25 μm.) (*D*) Simultaneous optical and electrophysiological recording of spontaneous activity in cell from *C*. The red trace is the hi-pass filtered VF2.1.Cl signal, sampled at 50 Hz. The black trace is the electrophysiological recording, sampled at 10 kHz. The optical trace shows near-perfect matching of the subthreshold membrane potential and a clear detectable signal indicating action potentials. Action potentials have variable amplitudes in the optical traces because of the relatively slow optical sampling rate (*SI Appendix*, Fig. S4).

display even faster kinetics, as forward charge shift occurs with absorbance, on the femtosecond time scale, and resolves itself upon emission of a photon, enabling these dyes to keep time with the fastest spiking neurons. FRET pair VSDs depend upon the migration of a lipophilic anion through an unstirred lipid bilayer and display kinetics in the millisecond-to-second time regime, limiting their application to monitoring only slow transients.

Because PeT shuttles an electron across the membrane and back on a microsecond or faster timescale, driven by photons rather than membrane potential changes, no capacitative loading should be observed. The same holds true for electrochromic dyes, which transfer electrons on even faster time scales. One disadvantage of electrochromic dyes is that they require the entire voltage-sensing chromophores to be rigid to enable π orbital overlap, quantum yield, efficient charge transfer, and maximization of voltage sensitivity (22). Such rigidity hinders synthesis and water solubility and may explain why electrochromic dyes are not improved by lengthening their chromophores. PeT probes do not require the entire molecular wire to be rigidly coplanar, and synthesis of longer wires is feasible.

PeT-sensing allows the entire emission spectrum to be used for monitoring voltage, because the quenching mechanism alters the Φ_{Fl}, decreasing the brightness of the dye, and does not shift the wavelength as do electrochromic methods. Because photons are not wasted, this allows lower intensity light to be used in experiments, reducing phototoxicity and increasing the duration of experimental procedures. The performance of electrochromic dyes has plateaued over four decades of development. Excitation at the far-red edge of the spectrum gives voltage sensitivities ranging from −35% to −52% ΔF/F per 100 mV; however, at the edge of the spectrum, the intensity is far below the peak and the voltage response becomes nonlinear (48).

Several limitations of the VF dyes remain to be addressed. VF derivatives are not yet genetically targetable. The sensors are readily taken up by the cell membranes of all tissue, increasing nonresponsive background fluorescence and decreasing the SNR. For heterogeneous preparations, such as intact leech ganglia and brain slices, this becomes an increasingly important issue, and one method to address this concern is through the genetic targeting of VSDs. VF sensors lend themselves to chemical derivatization, and efforts are underway to modify VF probes for targeting to genetically defined circuits of neurons.

Another drawback is that VF PeT sensors are not as sensitive to voltage as hoped. Our first derivatives show sensitivities ranging from 20–27% ΔF/F per 100 mV, and the most sensitive of existing electrochromic dyes exhibit −28% ΔF/F per 100-mV sensitivities in the linear range (47). Although it is encouraging that the first derivatives display sensitivities on a level approaching the most

Table 1. Summary of VSD attributes

Attribute	Electrochromic	FRET	PeT
Nature of translocating charge	Electron	Lipid soluble anion	Electron
Forward charge shift occurs when	Photon absorption	Membrane depolarization	Quenching
Reverse charge shift occurs when	Photon emission or radiationless decay	Membrane repolarization	Electron-hole recombination
Fractional charge x Fraction of total voltage	~0.1	0.4–0.6	~0.5
Δ energy for 100 mV ΔV	0.003–0.02 eV	0.06 eV	0.05 eV
Comparison energy	Photon energy 1.5–2 eV	kT 0.026 eV	kT 0.026 eV
Extended rigid fluorophore needed?	Yes	No	No
Use full ex/em band	No	Yes	Yes
Sensitivity Δ F/F per mV	Low	High	High
Speed	fs	ms–s	ns–μs
Capacitative loading	None	Significant	None

sensitive electrochromic dyes, we believe ample chemical space exists for improving the voltage sensitivity of molecular wire platforms. Because the voltage sensitivity is controlled by PeT, the efficiency of PeT can be rationally tuned (49) by altering the electron affinities of the donor, wire, and acceptor to maximize the fluorescence turn-on in response to depolarizations. Additionally, extending the molecular wire to span an even greater distance across the plasma membrane should increase sensitivity as the transferred electron samples more of the electric field. The modular nature of the VF synthesis allows for rapid interchange of coupling partners to quickly assemble and assess the voltage sensitivity of an array of compounds.

In summary, we present a unique method for monitoring voltage in neurons based on the voltage-sensitive PeT from an electron-rich donor to fluorescent reporter attached via a membrane-spanning molecular wire. The VF family of sensors have large, linear, turn-on fluorescence responses to depolarizing steps (20–27% $\Delta F/F$ per 100 mV), fast kinetics (τ <<140 μs), and negligible capacitative loading. VF2.4.Cl can detect and resolve evoked action potentials in primary culture hippocampal neurons, and VF2.1.Cl can monitor spontaneous spiking and synaptic potentials in leech Retzius cells with sensitivity and time-course essentially identical to the recorded electrophysiology signal. VF sensors provide a practical alternative to currently available VSDs, and future derivatives of the molecular wire platform will increase our ability to optically monitor the temporal and spatial dynamics of neuronal activity in defined circuits of neurons.

Methods

Imaging, electrophysiology, cell culture, leech imaging and electrophysiology, and data analysis methods are available in *SI Appendix*. Theoretical considerations of capacitative load are included in *SI Appendix*. Dyes were synthesized using standard synthetic procedures detailed in *SI Appendix*.

ACKNOWLEDGMENTS. We thank David Kleinfeld for use of a photomultiplier photometer and Intelligent Imaging Innovations and Photometrics for use of the Evolve 128 camera. This work was supported in part by the Howard Hughes Medical Institute and US National Institute of Neurological Disorders and Stroke Grant R37 NS027177 (to R.Y.T.); National Institutes of Health Grant MH43396 and National Science Foundation Grant IOB-0523959 (to W.B.K.); the National Institute of Biomedical Imaging and Bioengineering for Postdoctoral Fellowship F32 EB012423 (to E.W.M.); and National Institutes of Health Training Grants EB009380 and MH020002 (to E.P.F.).

1. Scanziani M, Häusser M (2009) Electrophysiology in the age of light. *Nature* 461: 930–939.
2. Peterka DS, Takahashi H, Yuste R (2011) Imaging voltage in neurons. *Neuron* 69:9–21.
3. Poenie M, Alderton J, Tsien RY, Steinhardt RA (1985) Changes of free calcium levels with stages of the cell division cycle. *Nature* 315:147–149.
4. Tsien RY, Rink TJ, Poenie M (1985) Measurement of cytosolic free Ca2+ in individual small cells using fluorescence microscopy with dual excitation wavelengths. *Cell Calcium* 6:145–157.
5. Grynkiewicz G, Poenie M, Tsien RY (1985) A new generation of Ca2+ indicators with greatly improved fluorescence properties. *J Biol Chem* 260:3440–3450.
6. Minta A, Kao JP, Tsien RY (1989) Fluorescent indicators for cytosolic calcium based on rhodamine and fluorescein chromophores. *J Biol Chem* 264:8171–8178.
7. Nagai T, Sawano A, Park ES, Miyawaki A (2001) Circularly permuted green fluorescent proteins engineered to sense Ca2+. *Proc Natl Acad Sci USA* 98:3197–3202.
8. Miyawaki A, et al. (1997) Fluorescent indicators for Ca2+ based on green fluorescent proteins and calmodulin. *Nature* 388:882–887.
9. Tian L, et al. (2009) Imaging neural activity in worms, flies and mice with improved GCaMP calcium indicators. *Nat Methods* 6:875–881.
10. Mank M, et al. (2008) A genetically encoded calcium indicator for chronic in vivo two-photon imaging. *Nat Methods* 5:805–811.
11. Heim N, Griesbeck O (2004) Genetically encoded indicators of cellular calcium dynamics based on troponin C and green fluorescent protein. *J Biol Chem* 279: 14280–14286.
12. Palmer AE, et al. (2006) Ca2+ indicators based on computationally redesigned calmodulin-peptide pairs. *Chem Biol* 13:521–530.
13. Horikawa K, et al. (2010) Spontaneous network activity visualized by ultrasensitive Ca (2+) indicators, yellow Cameleon-Nano. *Nat Methods* 7:729–732.
14. Cacciatore TW, et al. (1999) Identification of neural circuits by imaging coherent electrical activity with FRET-based dyes. *Neuron* 23:449–459.
15. González JE, Tsien RY (1997) Improved indicators of cell membrane potential that use fluorescence resonance energy transfer. *Chem Biol* 4:269–277.
16. González JE, Tsien RY (1995) Voltage sensing by fluorescence resonance energy transfer in single cells. *Biophys J* 69:1272–1280.
17. Sjulson L, Miesenböck G (2008) Rational optimization and imaging in vivo of a genetically encoded optical voltage reporter. *J Neurosci* 28:5582–5593.
18. Akemann W, Lundby A, Mutoh H, Knöpfel T (2009) Effect of voltage sensitive fluorescent proteins on neuronal excitability. *Biophys J* 96:3959–3976.
19. Wang D, Zhang Z, Chanda B, Jackson MB (2010) Improved probes for hybrid voltage sensor imaging. *Biophys J* 99:2355–2365.
20. Bradley J, Luo R, Otis TS, DiGregorio DA (2009) Submillisecond optical reporting of membrane potential in situ using a neuronal tracer dye. *J Neurosci* 29:9197–9209.
21. Chanda B, et al. (2005) A hybrid approach to measuring electrical activity in genetically specified neurons. *Nat Neurosci* 8:1619–1626.
22. Hubener G, Lambacher A, Fromherz P (2003) Anellated hemicyanine dyes with large symmetrical solvatochromism of absorption and fluorescence. *J Phys Chem B* 107: 7896–7902.
23. Grinvald A (1983) Fluorescence monitoring of electrical responses from small neurons and their processes. *Biophys J* 42:195–198.
24. Fluhler E, Burnham VG, Loew LM (1985) Spectra, membrane binding, and potentiometric responses of new charge shift probes. *Biochemistry* 24:5749–5755.
25. Jacobs JM, Meyer T (1997) Control of action potential-induced Ca2+ signaling in the soma of hippocampal neurons by Ca2+ release from intracellular stores. *J Neurosci* 17: 4129–4135.
26. Davis WB, Svec WA, Ratner MA, Wasielewski MR (1998) Molecular-wire behaviour in p-phenylenevinylene oligomers. *Nature* 396:60–63.
27. de Silva AP, et al. (1995) New fluorescent model compounds for the study of photoinduced electron transfer: The influence of a molecular electric field in the excited state. *Angew Chem Int Ed Engl* 34:1728–1731.
28. Adams SR (2010) How calcium indicators work. *Cold Spring Harbor Protocols* 2010: pdb.top70.
29. de la Torre G, Giacalone F, Segura JL, Martín N, Guldi DM (2005) Electronic communication through pi-conjugated wires in covalently linked porphyrin/C60 ensembles. *Chemistry* 11:1267–1280.
30. Li LS (2007) Fluorescence probes for membrane potentials based on mesoscopic electron transfer. *Nano Lett* 7:2981–2986.
31. Garner LE, et al. (2010) Modification of the optoelectronic properties of membranes via insertion of amphiphilic phenylenevinylene oligoelectrolytes. *J Am Chem Soc* 132: 10042–10052.
32. Montana V, Farkas DL, Loew LM (1989) Dual-wavelength ratiometric fluorescence measurements of membrane potential. *Biochemistry* 28:4536–4539.
33. Briggman KL, Abarbanel HD, Kristan WB, Jr. (2005) Optical imaging of neuronal populations during decision-making. *Science* 307:896–901.
34. Salzberg BM, Grinvald A, Cohen LB, Davila HV, Ross WN (1977) Optical recording of neuronal activity in an invertebrate central nervous system: Simultaneous monitoring of several neurons. *J Neurophysiol* 40:1281–1291.
35. Ross WN, Arechiga H, Nicholls JG (1987) Optical recording of calcium and voltage transients following impulses in cell bodies and processes of identified leech neurons in culture. *J Neurosci* 7:3877–3887.
36. Taylor AL, Cottrell GW, Kleinfeld D, Kristan WB, Jr. (2003) Imaging reveals synaptic targets of a swim-terminating neuron in the leech CNS. *J Neurosci* 23:11402–11410.
37. Briggman KL, Kristan WB, Jr. (2006) Imaging dedicated and multifunctional neural circuits generating distinct behaviors. *J Neurosci* 26:10925–10933.
38. Baca SM, Marin-Burgin A, Wagenaar DA, Kristan WB, Jr. (2008) Widespread inhibition proportional to excitation controls the gain of a leech behavioral circuit. *Neuron* 57: 276–289.
39. Briggman KL, Kristan WB, Jr., Gonzalez JE, Kleinfeld D, Tsien RY (2010) Monitoring integrated activity of individual neurons using FRET-based voltage-sensitive dyes. *Membrane Potential Imaging in the Nervous System: Methods and Applications*, eds Canepari M, Zecevic D (Springer, New York), pp 61–70.
40. Ataka K, Pieribone VA (2002) A genetically targetable fluorescent probe of channel gating with rapid kinetics. *Biophys J* 82:509–516.
41. Perron A, et al. (2009) Second and third generation voltage-sensitive fluorescent proteins for monitoring membrane potential. *Front Mol Neurosci* 2:5.
42. Siegel MS, Isacoff EY (1997) A genetically encoded optical probe of membrane voltage. *Neuron* 19:735–741.
43. Kralj JM, Hochbaum DR, Douglass AD, Cohen AE (2011) Electrical spiking in *Escherichia coli* probed with a fluorescent voltage-indicating protein. *Science* 333:345–348.
44. Sjulson L, Miesenböck G (2007) Optical recording of action potentials and other discrete physiological events: A perspective from signal detection theory. *Physiology (Bethesda)* 22:47–55.
45. Fernández JM, Taylor RE, Bezanilla F (1983) Induced capacitance in the squid giant axon. Lipophilic ion displacement currents. *J Gen Physiol* 82:331–346.
46. Loew LM, Bonneville GW, Surow J (1978) Charge shift optical probes of membrane potential. Theory. *Biochemistry* 17:4065–4071.
47. Kuhn B, Fromherz P (2003) Anellated hemicyanine dyes in a neuron membrane: Molecular Stark effect and optical voltage recording. *J Phys Chem B* 107:7903–7913.
48. Kuhn B, Fromherz P, Denk W (2004) High sensitivity of Stark-shift voltage-sensing dyes by one- or two-photon excitation near the red spectral edge. *Biophys J* 87: 631–639.
49. Ueno T, et al. (2004) Rational principles for modulating fluorescence properties of fluorescein. *J Am Chem Soc* 126:14079–14085.